Biochemical and Biophysical Research Communications 448 (2014) 169–174

Contents lists available at ScienceDirect

Biochemical and Biophysical Research Communications

journal homepage: www.elsevier.com/locate/ybbrc

Crystal structure of the NHERF1 PDZ2 domain in complex with the chemokine receptor CXCR2 reveals probable modes of PDZ2 dimerization

Joshua Holcomb [a,1], Yuanyuan Jiang [a,1], Xiaoqing Guan [a,1], Laura Trescott [a], Guorong Lu [a], Yuning Hou [a], Shuo Wang [a], Joseph Brunzelle [b], Nualpun Sirinupong [c], Chunying Li [a,*], Zhe Yang [a,*]

[a] Department of Biochemistry and Molecular Biology, Wayne State University School of Medicine, Detroit, MI, USA
[b] Advanced Photon Source, Argonne National Lab, Argonne, IL, USA
[c] Nutraceuticals and Functional Food Research and Development Center, Prince of Songkla University, Hat-Yai, Songkhla, Thailand

ARTICLE INFO

Article history:
Received 12 April 2014
Available online 24 April 2014

Keywords:
NHERF1
CXCR2
X-ray crystallography
Scaffold protein
Dimerization
Neutrophil

ABSTRACT

The formation of CXCR2–NHERF1–PLCβ2 macromolecular complex in neutrophils regulates CXCR2 signaling and plays a key role in neutrophil chemotaxis and transepithelial neutrophilic migration. However, NHERF1 by itself, with only two PDZ domains, has a limited capacity in scaffolding the multiprotein-complex formation. Here we report the crystal structure of the NHERF1 PDZ2 domain in complex with the C-terminal CXCR2 sequence. The structure reveals that the PDZ2–CXCR2 binding specificity is achieved by numerous hydrogen bonds and hydrophobic contacts with the last four CXCR2 residues contributing to specific interactions. The structure also reveals two probable modes of PDZ2 dimerization where the two canonical ligand-binding pockets are well separated and orientated in a unique parallel fashion. This study provides not only the structural basis for the PDZ-mediated NHERF1–CXCR2 interaction, but also an additional example of how PDZ domains may dimerize, which both could prove valuable in understanding NHERF1 complex-scaffolding function in neutrophils.

1. Introduction

The chemokine receptor CXCR2 is a G-protein coupled receptor that plays important roles in regulating neutrophil chemotaxis and directing neutrophils to sites of inflammation [1,2]. Defective regulation of CXCR2 can cause excessive release of neutrophils from bone marrow and has been implicated in a variety of inflammatory diseases, including rheumatoid arthritis, psoriasis, inflammatory bowel disease, acute respiratory distress syndrome, septic shock, pulmonary emphysema, and chronic obstructive pulmonary disease [3]. Growing evidence suggests that CXCR2 interacts directly or indirectly with other receptors, ion channels, transporters, scaffolding proteins, effectors, and cytoskeletal elements to form macromolecular complexes at specialized subcellular domains [4,5]. These dynamic protein–protein interactions regulate CXCR2 signaling function as well as its localization and processing within cells [6,7]. We have shown that CXCR2, phospholipase C-β2 (PLCβ2), and Na^+/H^+ exchanger regulatory factor-1 (NHERF1) form macromolecular complexes at the plasma membrane of bone marrow neutrophil, which functionally couple chemokine signaling to PLCβ2-mediated signaling cascade [4]. We also showed that disruption of this NHERF1-bridged interaction abolishes CXCR2 signaling and inhibits neutrophil chemotaxis and transepithelial neutrophilic migration in vitro [4]. These findings imply that targeting the NHERF1-scaffolded CXCR2–PLCβ2 signaling cascade could provide new strategies for therapeutic interventions of CXCR2-related diseases.

The ability of NHERF1 to scaffold the formation of a multiprotein complex depends on its two PDZ (PSD-95/Discs-large/ZO-1) domains, PDZ1 and PDZ2. In general, PDZ domains mediate protein interactions by recognizing the C-terminal sequence of target proteins and binding to the targets through a canonically and structurally conserved PDZ peptide-binding pocket [8]. The specificity of the interactions is determined mainly by the residues at positions 0 and −2 of the peptides (position 0 referring to the C-terminal residue), whereas other residues do not significantly contribute to the interaction [8]. This has led to the classification of PDZ domains into two major specificity classes: type I, (S/T)X(V/I/L) (X denoting any amino acid); type II, (F/Y)X(F/V/A)

* Corresponding authors. Address: 540 E. Canfield Street, Detroit, MI 48201, USA. Fax: +1 313 577 2765.
E-mail addresses: cl@med.wayne.edu (C. Li), zyang@med.wayne.edu (Z. Yang).
[1] These authors contributed equally to this work.

http://dx.doi.org/10.1016/j.bbrc.2014.04.085
0006-291X/

[9,10]. The PDZ domains of NHERF1 are the type I PDZ domains that have been shown to be capable of interacting with many different proteins and robust in scaffolding multiprotein complex formation. In addition to CXCR2 and PLCβ2, the NHERF1 PDZ domains are able to interact with a range of other membrane and signaling proteins, such as cystic fibrosis transmembrane conductance regulator (CFTR), β2-adrenergic receptor (β2AR), platelet-derived growth factor receptor (PDGFR), and parathyroid hormone receptor (PTHR) [11]. Through these protein interactions, NHERF1 plays central roles in signaling complex assembly and receptor recycling as well as in establishing cell polarity and directing protein trafficking [8]. However, NHERF1 by itself, with only two PDZ domains, has a limited capacity to form multiprotein arrays or scaffold interactive proteins within membrane microdomains [12].

Notably, some PDZ domains, including the NHERF1 PDZ domains, can increase their scaffolding capacity through PDZ oligomerization with the same or different PDZ-containing proteins. Oligomerization of InaD through the third and fourth PDZ domains of separate InaD proteins has been shown to amplify the capacity and complexity of InaD-sequestered proteins in the Drosophila phototransduction networks [12]. Dimerization of ZO PDZ2 domains has been proposed to play a pivotal role in initiating claudin polymerization and directing tight junction strands for correct localization [13]. Analysis of over 150 PDZ domains in mouse genome revealed that 30% of mouse PDZ domains participate in PDZ–PDZ interactions, suggesting that many PDZ domains have evolved as a dual binding module in facilitating the formation of multiprotein complexes [14]. For NHERF1, both PDZ1 and PDZ2 can dimerize with homologous PDZ–PDZ interactions being more prominent than heterologous interactions [12]. The homodimerization of NHERF1 PDZs has been suggested to provide a mechanism for NHERF1 to expand its capacity in multiprotein complex assembly and regulating the activity of interacting proteins within membrane microdomains [12]. It should be noted that the PDZ1 and PDZ2 domains of NHERF1 exhibit distinct binding specificity: for example, both CXCR2 and PLCβ2 prefer to bind to PDZ2 [4,15]. It is conceivable that the assembly of the CXCR2–NHERF1–PLCβ2 signaling complex in neutrophils may not only require the PDZ canonical ligand-binding ability, but also the ability of NHERF1 to engage in separate PDZ–PDZ interactions. Consequently, such non-canonical PDZ-binding mode could have important implications in CXCR2–PLCβ2 coupling and in CXCR2-mediated neutrophil chemotaxis. In this context, we here present the crystal structure of NHERF1 PDZ2 in complex with the CXCR2 C-terminal peptide TSTTL. The structure reveals the PDZ2–CXCR2 interaction specificity and two probable modes of PDZ2 dimerization. The structure also suggests a model that the PDZ2 dimerization utilizes a distinct interface that functions together with two well-separated canonical ligand-binding pockets in scaffolding multiprotein complex formation.

2. Materials and methods

2.1. Protein expression and purification

A DNA fragment encoding the human NHERF1 PDZ2 (residues 155–234) was amplified by PCR using the full-length human NHERF1 cDNA as a template. The C-terminal extension TSTTL that corresponds to residues 356–360 of human CXCR2 was created by inclusion of 15 extra bases in the reverse primer. The PCR products were cloned in the pSUMO vector containing an N-terminal His6-SUMO tag. The resulting clone was transformed into *Escherichia coli* BL21 Condon Plus (DE3) cells for protein expression. The transformants were grown to an OD600 (optical density at 600 nm) of 0.4 at 37 °C in LB medium, and then induced with 0.1 mM isopropylthio-β-D-galactoside at 15 °C overnight. The cells were harvested by centrifugation and lysed by French Press. The soluble fraction was then subjected to Ni^{2+} affinity chromatography purification, followed by the cleavage of the His6-SUMO tag with yeast SUMO Protease 1. PDZ2 proteins were separated from the cleaved tag by a second Ni^{2+} affinity chromatography and further purified by size-exclusion chromatography. Finally, the proteins were concentrated to 10–20 mg/ml in a buffer containing 20 mM Tris–HCl (pH 8.0), 150 mM NaCl, 1 mM β-mercaptoethanol, and 5% glycerol.

2.2. Crystallization, data collection and structure determination

Crystals were grown by the hanging-drop vapor-diffusion method by mixing the protein (~20 mg/ml) with an equal volume of a reservoir solution containing 100 mM Tris–HCl, pH 8.5, 8% PEG8000 at 20 °C. Crystals typically appeared overnight and continued to grow to their full size in 2–3 days. Prior to X-ray diffraction data collection, crystals were cryoprotected in a solution containing the mother liquor and 25% glycerol and flash cooled in liquid nitrogen. The data were collected at 100 K at beamline 21-ID-F at the Advanced Photon Source (Argonne, IL) and processed and scaled using the program XDS [16]. Crystals belong to the space group $P2_1$ with two molecules in the asymmetric unit (Table 1). The structure was solved by the molecular replacement method with the program PHASER [17] using the PDZ2–TETSL structure (PDB code: 2OZF) as a search model. Structure modeling was carried out in COOT [18], and refinement was performed with PHENIX [19]. To reduce the effects of model bias,

Table 1
Crystallographic data and refinement statistics.

Data	
Space group	$P2_1$
Cell parameters	
a, *b*, *c* (Å)	32.8, 55.3, 54.2
β (°)	90.7
Wavelength (Å)	0.97856
Resolution (Å)	32.8-1.44 (1.49-1.44)
R_{merge}[a]	0.042 (0.369)[b]
Redundancy	3.5 (2.7)
Unique reflections	28,239
Completeness (%)	96.8 (78.2)
$\langle I/\sigma \rangle$	17.8 (2.3)
Refinement	
Resolution (Å)	32.8–1.44 (1.49–1.44)
Molecules/AU	2
R_{work}[c]	0.166 (0.254)
R_{free}[d]	0.197 (0.304)
Ramachandran plot	
Residues in favored	98.3%
Residues in allowed	1.7%
RMSD	
Bond lengths (Å)	0.007
Bond angels (°)	1.12
No. of atoms	
Protein	1299
Peptide	72
Water	249
B-factor (Å^2)	
Protein	24.1
Peptide	20.2
Water	33.4

[a] $R_{merge} = \Sigma|I - \langle I \rangle|/\Sigma I$, where I is the observed intensity and $\langle I \rangle$ is the averaged intensity of multiple observations of symmetry-related reflections.
[b] Numbers in parentheses refer to the highest resolution shell.
[c] $R_{work} = \Sigma|F_o - F_c|/\Sigma|F_o|$, where F_o is the observed structure factor, F_c is the calculated structure factor.
[d] R_{free} was calculated using a subset (5%) of the reflection not used in the refinement.

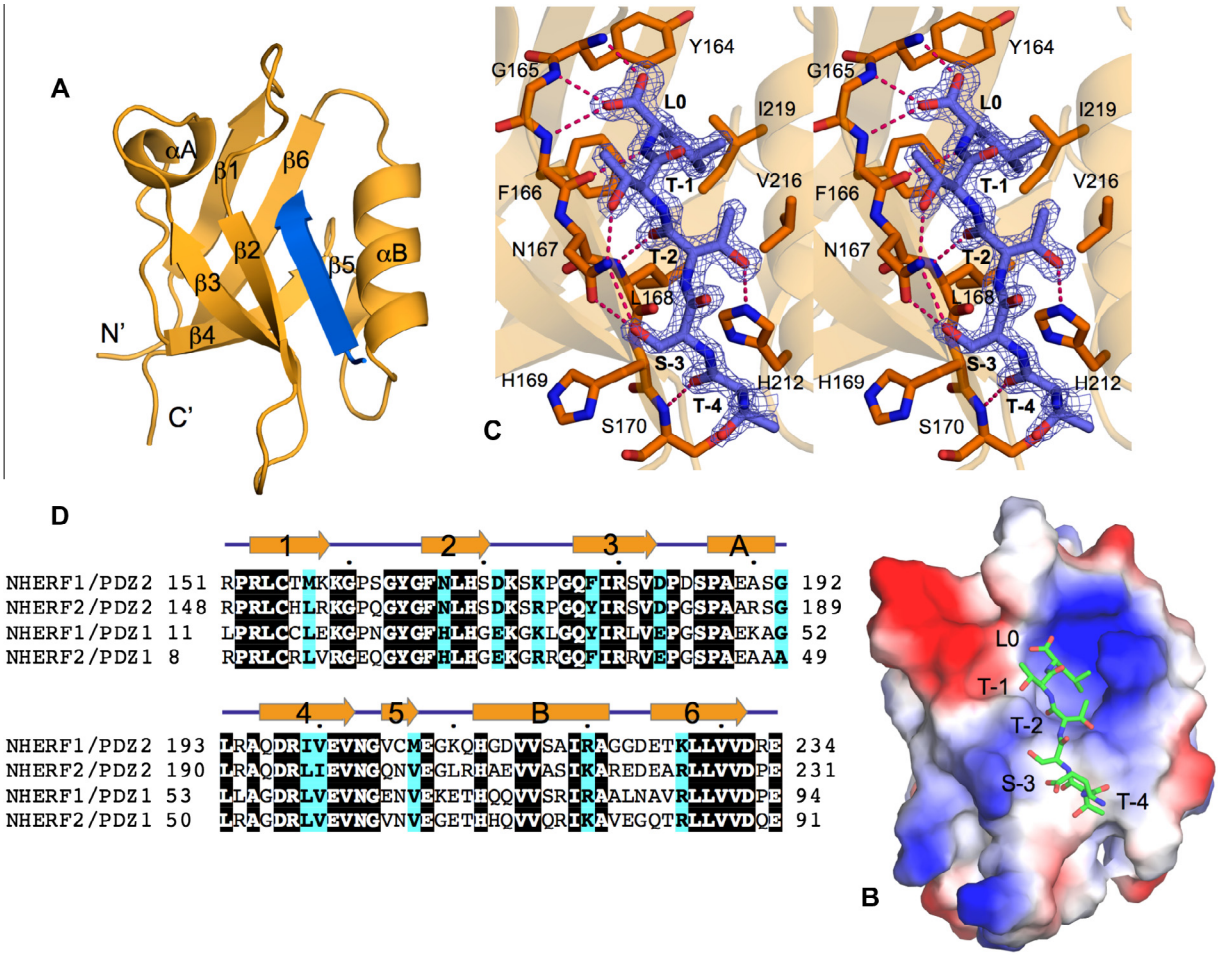

Fig. 1. Structure of NHERF1 PDZ2 in complex with the CXCR2 C-terminal sequence TSTTL. (A) Ribbon diagram of the PDZ2–CXCR2 structure. PDZ2 is shown in orange and the CXCR2 peptide is shown in blue. Secondary structures of PDZ2, α-helices, and β-strands are labeled and numbered according to their position in the sequence. (B) Surface representation of the PDZ2–CXCR2 structure. Surface coloring is according to the electrostatic potential: red, white, and blue correspond to negative, neutral, and positive potential, respectively. The vacuum electrostatics/protein contact potential was generated by PyMOL. The CXCR2 peptide is depicted by sticks. (C) Stereo view of the PDZ2 ligand-binding site bound to the CXCR2 C-terminal peptide. PDZ2 residues are represented by sticks with their carbon atoms colored in orange. The CXCR2 peptide is depicted by sticks overlaid with $2F_o - F_c$ omit map calculated at 1.44 Å and contoured at 1.8 σ. Hydrogen bonds are illustrated as red broken lines. (D) Sequence alignment of selected PDZ domains. The alignment was performed by ClustalW [30], including human NHERF1 and NHERF2. Identical residues are shown as white on black, and similar residues appear shaded in cyan. Secondary structure elements are displayed above the sequences and labeled according to the scheme in A. Sequence numbering is displayed to the left of the sequences, with every 10th residue marked by a dot shown above the alignment. (For interpretation of the references to color in this figure legend, the reader is referred to the web version of this article.)

iterative-build OMIT maps were used during model building and structure refinement. The final models were analyzed and validated with Molprobity [20]. All figures of 3D representations of the PDZ2–CXCR2 structure were made with PyMOL (www.pymol.org).

2.3. Protein data bank accession number

Coordinates and structure factors have been deposited in the Protein Data Bank with accession number 4Q3H.

3. Results and discussion

3.1. Structural basis of the PDZ2–CXCR2 interaction

The overall structure of NHERF1 PDZ2 is similar to other PDZ domains [10,21], consisting of six β strands (β1–β6) and two α-helices (αA and αB) (Fig. 1A and B). The CXCR2 peptide binds in the cleft between β2 and αB, burying a total solvent-accessible surface area of 649 Å^2. The binding specificity of the PDZ2–CXCR2 interaction is achieved through networks of hydrogen bonds and hydrophobic interactions (Fig. 1C). At the ligand position 0, the side chain of Leu0 is nestled in a deep hydrophobic pocket formed by invariant residues Tyr164, Phe166, and Leu168 from β2 and Val216 and Ile219 from αB (Fig. 1D). In the pocket, the position of Leu0 is further secured by both a hydrogen bond from its amide nitrogen to the Phe166 carbonyl oxygen and triplet hydrogen bonding between the Leu0 carboxylate and the amides of Tyr164, Gly165, and Phe166. Similar interactions have been observed in several other PDZ-mediated complexes [10,21], which represent the most-conserved binding mode for terminal Leu recognition. Residues at other peptide positions also contribute to the PDZ2–CXCR2 complex formation (Fig. 1C). At position −1, the side chain hydroxyl of Thr-1 forms a hydrogen bond with the Nδ2 atom of the Asn167 side chain. At position −2, Thr-2 makes one hydrogen bond to the His212 imidazole group and two hydrogen bonds to the highly conserved residue Leu168. At the ligand position −3, the interactions with Ser-3 include one hydrogen bond from its side chain hydroxyl to the Oδ1 atom of Asn167, and another hydrogen bond to the Nδ1 atom of Asn167. The latter two interactions represent PDZ2 specific interactions, as Ser-3 recognition in

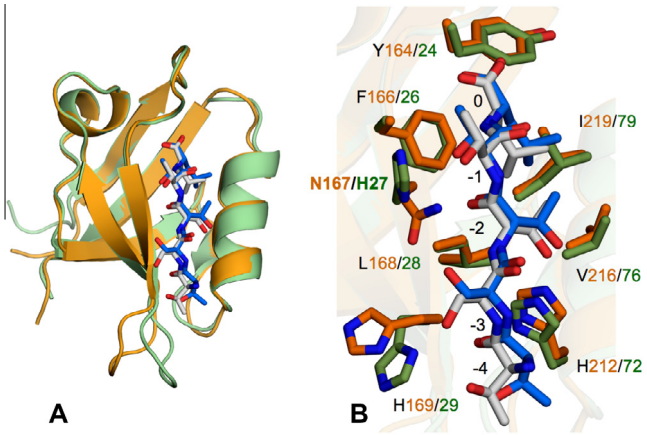

Fig. 2. Structural comparison of NHERF1 PDZ2 and PDZ1. (A) Superposition of the structures of PDZ2–CXCR2 (orange–blue; PDB code: 4Q3H) and PDZ1–CXCR2 (green–gray; PDB code: 4JL7). PDZ domains are represented by ribbons. Residues in the ligands are displayed as sticks. (B) Superposition of the PDZ ligand-binding pockets. Both PDZ and ligand residues are depicted by sticks and colored according to the scheme in A. (For interpretation of the references to color in this figure legend, the reader is referred to the web version of this article.)

PDZ1–CXCR2 is mediated by an His residue at His169 position [22]. Finally, the peptide residue Thr-4 engages in a main-chain contact with Ser170, but does not participate in any specific side-chain interactions. These observations indicate that the last four residues of CXCR2 contribute to the binding specificity in the PDZ2–CXCR2 complex formation.

3.2. Differential CXCR2 interaction with PDZ1 and PDZ2

To gain further insight into PDZ2 binding specificity, we compared the PDZ2–CXCR2 structure to the structure of the NHERF1 PDZ1–CXCR2 complex. The overall structures of the two liganded PDZs are very similar, with a root mean square difference (RMSD) of 1.02 Å for 83 Cα atoms (Fig. 2A). The main chains of the bound peptides superimpose well (RMSD of 0.15 Å), as do their relative spatial positions to the conserved PDZ motifs. In addition, the ligand recognition modes at the peptide positions 0 and −2 are virtually indistinguishable, characterized by structurally similar binding sites composed with completely conserved residues (Figs. 2B and 1D). However, substantial differences are observed in the ligand recognition at positions −1 and −3. Note these differences are associated directly with the only residue difference in their peptide-binding pockets. In PDZ1, the residue His at position 27 is replaced by Asn at the matching position (167) in PDZ2. As a result of this difference, Thr-1 does not hydrogen bond to the His27 side chain in PDZ1, instead of forming a general, rather ligand-indiscriminative Van der Waals interaction (Fig. 2B). At position −3, no direct contacts are observed between Ser-3 and His27 in PDZ1–CXCR2. This contrasts to the PDZ2–CXCR2 complex where the side chain of Asn167 adopts a different rotamer that allows direct hydrogen bonding with the Ser-3 hydroxyl (Fig. 1C). Specific interaction of Ser-3 with Asn167 in PDZ2–CXCR2, but not with His27 in PDZ1–CXCR2, is consistent with previous affinity selection experiments in which PDZ2 almost exclusively selected ligands with Ser at position −3 from random peptides, whereas PDZ1 showed no apparent preference for this position [23].

3.3. Two probable modes of PDZ2 dimerization

Both NHERF1 PDZ1 and PDZ2 can dimerize, and their dimerization has been suggested to facilitate the formation of multiprotein complexes and contributes to NHERF1-mediated intracellular signaling [12]. However, the molecular details of NHERF1 PDZ dimerization are unknown. Examination of the crystal packing reveals two probable modes of PDZ2 dimerization. As shown in Fig. 3A and B, both dimers are generated by a twofold symmetry. Dimer 1 is generated by the parallel stacking of helix αB from both monomers, while dimer 2 is generated by the interactions between two copies of strands β1, β4, and β6. In dimer 1, the buried surface area at the dimer interface is 497 Å^2, which is comparable to

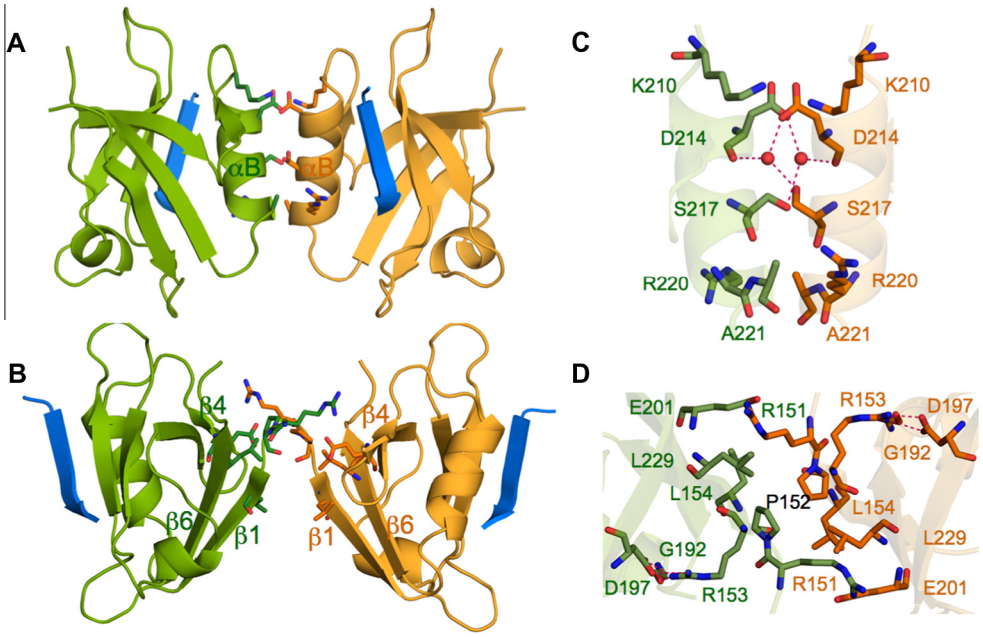

Fig. 3. Two probable modes of PDZ2 dimerization. (A) Overall view of dimer 1 and (B) dimer 2. (C) Close-up view of the interactions in dimer 1 and (D) dimer 2. PDZ backbones are represented by ribbons with monomers colored green and orange. CXCR2 peptides are depicted by ribbons and shown in blue. Interacting residues at the dimer interface are depicted by sticks. Secondary structural elements are marked as in Fig. 1A. (For interpretation of the references to color in this figure legend, the reader is referred to the web version of this article.)

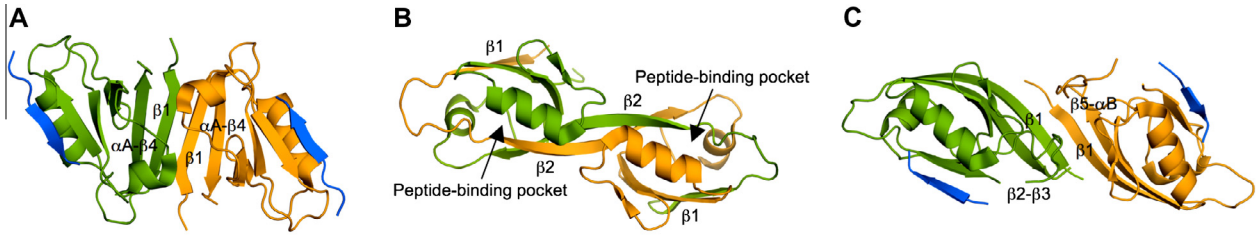

Fig. 4. Structural diversity in PDZ dimerization. Ribbon representation of the (A) GRIP PDZ6 dimer (PDB code: 1N7F), (B) ZO PDZ2 dimer (PDB code: 2RCZ), and (C) SHANK PDZ dimer (PDB code: 1Q3P). PDZ monomers are shown in green and orange. Target peptides are shown in blue. Structural elements involved in PDZ dimerization are indicated. (For interpretation of the references to color in this figure legend, the reader is referred to the web version of this article.)

592 Å^2 calculated for dimer 2. However, residues that form the dimer interface are only conserved in dimer 2 but not in dimer 1 (Figs. 3 and 1D). For dimer 1, the interactions at the interface include a salt-bridge between Lys210 and Asp214, two water-mediated hydrogen bonds between Asp214 and Ser217, and three stacking interactions involving Asp214, Ser217, Arg220, and Ala221 (Fig. 3C). Because this interface is based on the twofold symmetry, the intermolecular interactions are contributed in the same way by both monomers in stabilizing the dimer structure. For dimer 2, the interactions at the interface include a salt bridge between Arg151 and Glu201 and the hydrophobic interactions between Pro152, Leu154, and Leu229 from both monomers (Fig. 3D). Although Arg153 is not directly involved in this interface, its side chain guanidinium makes three intramolecular hydrogen bonds to Asp197 and Gly192, which stabilize the conformation of the interface-forming β1 strand in dimer 2. It is of particular interest to note that NHERF1 R153Q mutation was recently found in patients who have impaired renal phosphate reabsorption [24]. Subsequent studies demonstrated that this disease mutation abolished NHERF1 dimerization but did not disrupt its interaction with the parathyroid hormone 1 receptor [25]. While future studies are required to demonstrate the biological significance of the crystallographically observed dimerization, the high degree of conservation and the close proximity of the disease-related mutation suggest that the interface observed in dimer 2 might have some physiological relevance. In this regard, only dimer-2 model is considered further.

In dimer 2, the canonical target-binding pockets are located at the distal sides of the dimer interface. They are arranged in a parallel fashion and related by the same twofold symmetry present at the dimer interface (Fig. 3B). In the dimer, the CXCR2 peptides are clearly resolved in both pockets, with the binding conformations highly similar to those observed in the monomeric PDZ–ligand complexes (Fig. 2A). This indicates that the dimerization does not affect the PDZ2–peptide binding in the crystal, or the binding sites in the dimer are open to allow the interaction with the target proteins. This observation is also consistent with the previously proposed model that PDZ dimerization utilizes a distinct interface that functions together with two well-separated canonical ligand-binding pockets in scaffolding multiprotein complex formation [26].

3.4. Structural diversity in PDZ dimerization

In addition to the NHERF1 PDZ domains, other PDZ domains capable of dimerization include GRIP (glutamate receptor interacting protein) PDZ6, SHANK (SH3 and multiple ankyrin repeat domains protein) PDZ, and ZO (zonula occludens protein) PDZ2 [27–29]. Like NHERF1 oligomerization, the ability of these PDZ domains to dimerize has been suggested to expand PDZ scaffolding capacity and facilitate the formation of multiprotein complexes [26]. In line with this suggestion, recent family-wide proteomic investigation demonstrated that PDZ dimerization is surprisingly abundant, with ~30% mouse PDZ domains engaging in PDZ–PDZ interactions [14]. Interestingly, PDZ–PDZ interactions appear to be substantially more selective than interactions between PDZ domains and the C termini of their target proteins [14]. Modeling studies based on large-scale binding data predicted that one PDZ domain, on average, interacts with 245 different proteins via C-termini, contrasting only 1.7 PDZ domains via dimerization [14]. This suggests that the non-canonical binding mode contributes more to defining the precise composition of protein complexes than does the canonical binding mode [14].

Structurally, the high selectivity of PDZ–PDZ interactions is manifested by highly distinct dimerization modes and substantially different dimer interfaces. For example, in GRIP PDZ6, the dimer interface is formed primarily by the N-terminal β1 strand and parts of the β4–αA loop, whereas in ZO PDZ2 domain, the dimerization occurs via a domain-swapping mechanism, with β1 and β2 protruding out and exchanged between two symmetry-related monomers (Fig. 4). In contrast, the dimer interface in SHANK PDZ involves both β1 and two distinct loops of β2–β3 and β5–αB, which effectively define a new mode of PDZ dimerization. It is also interesting to note that the orientation of two canonical ligand-binding pockets in the NHERF1 PDZ2 dimer is unique among the known PDZ structures. In NHERF1 PDZ2, the ligands are orientated parallelly, whereas in other PDZ dimers the two ligands are positioned in an antiparallel fashion (Figs. 3B and 4). Therefore, these observed differences demonstrate the structural diversity in PDZ dimerization, consistent with prior suggestion that diverse PDZ–PDZ interactions have been optimized as a mechanism in scaffolding the formation of distinct multiprotein complexes [14]. This also highlights the potential importance of the present study, as it provides an additional example of how PDZ domains may dimerize and could be valuable in understanding NHERF1 complex-scaffolding function in neutrophils and also in CXCR2-related diseases.

Acknowledgments

This study was supported by the Leukemia Research Foundation, Aplastic Anemia & MDS International Foundation, and American Heart Association Grant number 0835085N (to Z.Y.) and from the Elsa U. Pardee Foundation, American Heart Association, and American Cancer Society Institutional Research Grant #11-053-01-IRG (to C.L.).

References

[1] R.W. Chapman, J.E. Phillips, R.W. Hipkin, A.K. Curran, D. Lundell, J.S. Fine, CXCR2 antagonists for the treatment of pulmonary disease, Pharmacol. Ther. 121 (2009) 55–68.
[2] H.H. Tsai, E. Frost, V. To, S. Robinson, C. Ffrench-Constant, R. Geertman, R.M. Ransohoff, R.H. Miller, The chemokine receptor CXCR2 controls positioning of oligodendrocyte precursors in developing spinal cord by arresting their migration, Cell 110 (2002) 373–383.

[3] W. Gonsiorek, X. Fan, D. Hesk, J. Fossetta, H. Qiu, J. Jakway, M. Billah, M. Dwyer, J. Chao, G. Deno, A. Taveras, D.J. Lundell, R.W. Hipkin, Pharmacological characterization of Sch527123, a potent allosteric CXCR1/CXCR2 antagonist, J. Pharmacol. Exp. Ther. 322 (2007) 477–485.
[4] Y. Wu, S. Wang, S.M. Farooq, M.P. Castelvetere, Y. Hou, J.L. Gao, J.V. Navarro, D. Oupicky, F. Sun, C. Li, A chemokine receptor CXCR2 macromolecular complex regulates neutrophil functions in inflammatory diseases, J. Biol. Chem. 287 (2012) 5744–5755.
[5] S. Wang, Y. Wu, Y. Hou, X. Guan, M.P. Castelvetere, J.J. Oblak, S. Banerjee, T.M. Filtz, F.H. Sarkar, X. Chen, B.P. Jena, C. Li, CXCR2 macromolecular complex in pancreatic cancer: a potential therapeutic target in tumor growth, Transl. Oncol. 6 (2013) 216–225.
[6] A.C. Magalhaes, H. Dunn, S.S. Ferguson, Regulation of GPCR activity, trafficking and localization by GPCR-interacting proteins, Br. J. Pharmacol. 165 (2012) 1717–1736.
[7] N.F. Neel, M. Barzik, D. Raman, T. Sobolik-Delmaire, J. Sai, A.J. Ham, R.L. Mernaugh, F.B. Gertler, A. Richmond, VASP is a CXCR2-interacting protein that regulates CXCR2-mediated polarization and chemotaxis, J. Cell Sci. 122 (2009) 1882–1894.
[8] B.Z. Harris, W.A. Lim, Mechanism and role of PDZ domains in signaling complex assembly, J. Cell Sci. 114 (2001) 3219–3231.
[9] M. Sheng, C. Sala, PDZ domains and the organization of supramolecular complexes, Annu. Rev. Neurosci. 24 (2001) 1–29.
[10] S. Karthikeyan, T. Leung, J.A. Ladias, Structural basis of the Na^+/H^+ exchanger regulatory factor PDZ1 interaction with the carboxyl-terminal region of the cystic fibrosis transmembrane conductance regulator, J. Biol. Chem. 276 (2001) 19683–19686.
[11] J.A. Ardura, P.A. Friedman, Regulation of G protein-coupled receptor function by Na^+/H^+ exchange regulatory factors, Pharmacol. Rev. 63 (2011) 882–900.
[12] L. Fouassier, C.C. Yun, J.G. Fitz, R.B. Doctor, Evidence for ezrin-radixin-moesin-binding phosphoprotein 50 (EBP50) self-association through PDZ–PDZ interactions, J. Biol. Chem. 275 (2000) 25039–25045.
[13] K. Umeda, J. Ikenouchi, S. Katahira-Tayama, K. Furuse, H. Sasaki, M. Nakayama, T. Matsui, S. Tsukita, M. Furuse, ZO-1 and ZO-2 independently determine where claudins are polymerized in tight-junction strand formation, Cell 126 (2006) 741–754.
[14] B.H. Chang, T.S. Gujral, E.S. Karp, R. BuKhalid, V.P. Grantcharova, G. MacBeath, A systematic family-wide investigation reveals that ~30% of mammalian PDZ domains engage in PDZ–PDZ interactions, Chem. Biol. 18 (2011) 1143–1152.
[15] C. Sun, D.F. Mierke, Characterization of interactions of Na^+/H^+ exchanger regulatory factor-1 with the parathyroid hormone receptor and phospholipase C, J. Pept. Res. 65 (2005) 411–417.
[16] W. Kabsch, Xds, Acta Crystallogr. D Biol. Crystallogr. 66 (2010) 125–132.
[17] A.J. McCoy, R.W. Grosse-Kunstleve, P.D. Adams, M.D. Winn, L.C. Storoni, R.J. Read, Phaser crystallographic software, J. Appl. Crystallogr. 40 (2007) 658–674.
[18] P. Emsley, K. Cowtan, Coot: model-building tools for molecular graphics, Acta Crystallogr. D Biol. Crystallogr. 60 (2004) 2126–2132.
[19] P.D. Adams, P.V. Afonine, G. Bunkoczi, V.B. Chen, I.W. Davis, N. Echols, J.J. Headd, L.W. Hung, G.J. Kapral, R.W. Grosse-Kunstleve, A.J. McCoy, N.W. Moriarty, R. Oeffner, R.J. Read, D.C. Richardson, J.S. Richardson, T.C. Terwilliger, P.H. Zwart, PHENIX: a comprehensive Python-based system for macromolecular structure solution, Acta Crystallogr. D Biol. Crystallogr. 66 (2010) 213–221.
[20] V.B. Chen, W.B. Arendall 3rd, J.J. Headd, D.A. Keedy, R.M. Immormino, G.J. Kapral, L.W. Murray, J.S. Richardson, D.C. Richardson, MolProbity: all-atom structure validation for macromolecular crystallography, Acta Crystallogr. D Biol. Crystallogr. 66 (2010) 12–21.
[21] S.T. Runyon, Y. Zhang, B.A. Appleton, S.L. Sazinsky, P. Wu, B. Pan, C. Wiesmann, N.J. Skelton, S.S. Sidhu, Structural and functional analysis of the PDZ domains of human HtrA1 and HtrA3, Protein Sci. 16 (2007) 2454–2471.
[22] G. Lu, Y. Wu, Y. Jiang, S. Wang, Y. Hou, X. Guan, J. Brunzelle, N. Sirinupong, S. Sheng, C. Li, Z. Yang, Structural insights into neutrophilic migration revealed by the crystal structure of the chemokine receptor CXCR2 in complex with the first PDZ domain of NHERF1, PLoS ONE 8 (2013) e76219.
[23] S. Wang, R.W. Raab, P.J. Schatz, W.B. Guggino, M. Li, Peptide binding consensus of the NHE-RF-PDZ1 domain matches the C-terminal sequence of cystic fibrosis transmembrane conductance regulator (CFTR), FEBS Lett. 427 (1998) 103–108.
[24] Z. Karim, B. Gerard, N. Bakouh, R. Alili, C. Leroy, L. Beck, C. Silve, G. Planelles, P. Urena-Torres, B. Grandchamp, G. Friedlander, D. Prie, NHERF1 mutations and responsiveness of renal parathyroid hormone, N. Engl. J. Med. 359 (2008) 1128–1135.
[25] B. Wang, C.K. Means, Y. Yang, T. Mamonova, A. Bisello, D.L. Altschuler, J.D. Scott, P.A. Friedman, Ezrin-anchored protein kinase A coordinates phosphorylation-dependent disassembly of a NHERF1 ternary complex to regulate hormone-sensitive phosphate transport, J. Biol. Chem. 287 (2012) 24148–24163.
[26] J. Chen, L. Pan, Z. Wei, Y. Zhao, M. Zhang, Domain-swapped dimerization of ZO-1 PDZ2 generates specific and regulatory connexin43-binding sites, EMBO J. 27 (2008) 2113–2123.
[27] Y.J. Im, S.H. Park, S.H. Rho, J.H. Lee, G.B. Kang, M. Sheng, E. Kim, S.H. Eom, Crystal structure of GRIP1 PDZ6–peptide complex reveals the structural basis for class II PDZ target recognition and PDZ domain-mediated multimerization, J. Biol. Chem. 278 (2003) 8501–8507.
[28] Y.J. Im, J.H. Lee, S.H. Park, S.J. Park, S.H. Rho, G.B. Kang, E. Kim, S.H. Eom, Crystal structure of the Shank PDZ–ligand complex reveals a class I PDZ interaction and a novel PDZ–PDZ dimerization, J. Biol. Chem. 278 (2003) 48099–48104.
[29] A.S. Fanning, M.F. Lye, J.M. Anderson, A. Lavie, Domain swapping within PDZ2 is responsible for dimerization of ZO proteins, J. Biol. Chem. 282 (2007) 37710–37716.
[30] M.A. Larkin, G. Blackshields, N.P. Brown, R. Chenna, P.A. McGettigan, H. McWilliam, F. Valentin, I.M. Wallace, A. Wilm, R. Lopez, J.D. Thompson, T.J. Gibson, D.G. Higgins, Clustal W and Clustal X version 2.0, Bioinformatics 23 (2007) 2947–2948.